Biochemical Pharmacology, Vol. 58, pp. 1155–1166, 1999.

ISSN 0006-2952/99/$–see front matter
PII S0006-2952(99)00196-3

Biochemical and Functional Characterization of Nitric Oxide Synthase III Gene Transfer Using a Replication-Deficient Adenoviral Vector

Armin Frey, Sonja Schneider-Rasp,† Uta Marienfeld,† Julie C.-M. Yu,‡ Martin Paul,§ Wolfgang Poller‡ and Harald H. H. W. Schmidt*‖*

*Department of Pharmacology and Toxicology and †Departmment of Clinical Biochemistry and Pathobiochemistry, Julius-Maximilians-University, D-97078 Würzburg; and ‡Department for Cardiology and Pneumology and §Department of Clinical Pharmacology and Toxicology, University Hospital Benjamin Franklin, Freie Universitat, D-12200 Berlin, Germany

ABSTRACT. Nitric oxide (NO) produced in endothelial cells has been implicated in the regulation of blood pressure, regional blood flow, inhibition of platelet aggregation, and endothelial and vascular smooth muscle cell proliferation. In a variety of cardiovascular disease states, such as atherosclerosis, arterial hypertension, and restenosis, expression of endothelial NO synthase (NOS-III) and endothelial NO production appear to be altered. Thus, NOS-III is an attractive target for cardiovascular gene therapy for which adenoviral vectors are one of the most effective vector systems. Therefore, a recombinant adenoviral vector expressing NOS-III (adenovirus type 5 [Ad5] cytomegalovirus [CMV] NOSIII) was constructed and biochemically and pharmacologically characterized both *in vitro* and in intact cells. Ad5CMVNOSIII-derived recombinant NOS-III was successfully expressed, as shown by immunoprecipitation and immunocytochemistry, and biologically active, as shown by functional assays in human primary umbilical vein and EA.hy926 endothelial cells, as well as 293 human embryonic kidney and Chinese hamster ovary cells. The K_m values for NADPH and L-arginine and the K_a for tetrahydrobiopterin as well as the enzyme's dependency on other cofactors were similar to recombinant reference enzyme and literature values. NOS-III expression levels correlated linearly with the multiplicity of infection with Ad5CMVNOSIII and lasted for at least 8 days. NOS-III transfection inhibited endothelial cell proliferation. In conclusion, adenovirus-mediated gene transfer of Ad5CMVNOSIII to vascular and non-vascular cells resulted in the dose-dependent expression of intact, physiologically regulated, and functionally active NOS-III. BIOCHEM PHARMACOL **58**;7:1155–1166, 1999. © 1999 Elsevier Science Inc.

KEY WORDS. nitric oxide synthase; nitric oxide; adenoviral vectors; gene therapy; endothelial cells; adenovirus

The pathomechanism of several cardiovascular disease states is thought to involve perturbations of the short-term equilibrium between vasoconstriction and vasodilatation, and the long-term balance between cell migration/proliferation and quiescence. One of the key players which has been shown to exert complex effects on both functional and morphological vascular parameters is nitric oxide. NO¶ is the gaseous, enzymatic product of three distinct NO synthase isoforms (L-arginine, NADPH:oxygen oxidoreductases [nitric oxide-forming]; EC 1.14.13.39) and exerts its effects via activation of intracellular soluble guanylyl cyclase [1]. In addition to being a potent endogenous vasodilator, NO participates in the suppression of angiogenesis and inhibits proliferation of endothelial cells, as well as migration and proliferation of vascular smooth muscle cells, whilst overexpression of NOS-III reduces neointimal thickening in rat models of balloon injury [2]. NO has been implicated in the regulation of blood pressure and regional blood flow and inhibits platelet aggregation and leukocyte adherence [3]. Mice lacking endothelial NOS have elevated blood pressure [4, 5]. There is evidence that NOS-III is involved in essential hypertension, persistent pulmonary hypertension in newborns, and familial pregnancy-induced hypertension in women [6–8]. Abnormalities in endothelial NO production also occur in atherosclerosis, diabetes, thrombosis, and restenosis.

Replication-deficient recombinant adenoviruses are highly efficient and, thus, promising vectors for gene

‖ Corresponding author: Prof. Harald H. H. W. Schmidt, Department of Pharmacology and Toxicology, Julius-Maximilians-University, Versbacher Straße 9, D-97078 Würzburg, Germany. Tel. ++49 (0)931 201-3854; FAX ++49 (0)931 201-3539; E-mail: schmidt@toxi.uni-wuerzburg.de

¶ *Abbreviations:* Ad5, adenovirus type 5; CaM, calmodulin; CHO, Chinese hamster ovarian cells; CMV, cytomegalovirus; FAD, flavin adenine dinucleotide; FBS, fetal bovine serum; FITC, fluorescein isothiocyanate; FMN, flavin mononucleotide; H_4Bip, (1′*R*,2′*S*,6*R*)-5,6,7,8-tetrahydrobiopterin; HUVEC, human primary umbilical vein endothelial cells; LDH, lactate dehydrogenase; NO, nitric oxide; NOS, nitric oxide synthase; NOS-III, nitric oxide synthase type III; np, nucleotide position; PCR, polymerase chain reaction; p.i., post infectionem; PMSF, phenylmethylsulfonyl fluoride; and 293 cells, 293 human embryonic kidney cells.

Received 6 August 1998; accepted 26 April 1999.

transfer to blood vessel cells [9]. In contrast to other vector systems, such as retroviral vectors, they can infect both replicating and non-replicating cells, the latter being the predominant state of target cells in the vascular wall. In addition, "third-generation" adenoviral vectors have a very high packing capacity of up to 30 kb. In order to demonstrate the fully functional and physiologically regulated expression of an adenovector-derived recombinant NOS-III enzyme in endothelial cells for subsequent *in vivo* experiments, we developed and characterized an NOS-III vector and its biologically active product virologically, biochemically, and pharmacologically. Additionally, we investigated the effects of transgenic overexpression of NOS-III in human endothelial cells.

MATERIALS AND METHODS

Materials

FAD, glutathione, NADPH, and the Cytotoxicity Detection Kit were from Boehringer Mannheim; (1′*R*,2′*S*,6*R*)-5,6,7,8-tetrahydrobiopterin, from Schircks; L-[2,3,4,5-^{3}H]-arginine-HCl (specific activity $>$ 2.15 TBq/mmol), from Amersham; Trans35label, from ICN Biomedicals; Rotiszint eco plus, from Roth; FBS, OptiMEM, and lipofectamine, from Life Technologies; culture media, from BioWhittaker or Life Technologies. EN^{3}HANCE™ was from DuPont; AmpliTaq DNA Polymerase, from Applied Biosystems–Perkin Elmer. SDS-PAGE gels (4–15% gradient) were purchased from BioRad; affinity-purified polyclonal rabbit anti-human NOS-III antiserum, from Transduction Labs; FITC-conjugated goat anti-rabbit immunoglobulin G antiserum, from Sigma; and pJM17, from Microbix Biosystem. Ad5CMVluc firefly luciferase adenovector was a kind gift from Bob Gerad, University of Texas Southwest Medical Centre (Dallas, TX, U.S.A.). NOS-III cDNA was a generous gift from T. Michel, Harvard Medical School (Boston, MA, U.S.A.). All other chemicals were either from Sigma or Merck.

Cell Culture

293 cells were grown in Dulbecco's modified Eagle's medium containing 4.5 g L^{-1} glucose, 10% FBS, 100 IU mL^{-1} penicillin, and 100 μg mL^{-1} streptomycin. HUVEC were isolated from human umbilical veins by a method described previously [9]. The umbilical cord vein was rinsed with PBS, filled with 20–30 mL of 0.1% collagenase solution, and incubated for 15 min (37°, 5% CO_2, 95% humidity). Cells were then rinsed from the vein with PBS, pelleted at 250 *g*, resuspended in serum-containing medium, and plated in culture flasks coated with gelatin. The cells were washed with PBS and fed with fresh medium every second day. When the primary culture reached confluence, cells were trypsinized and split into two flasks. Upon confluence, the cells from these flasks were again trypsinized and plated to 12 culture dishes (6-cm diameter), which were then used for the experiments. For the HUVEC cultures, we used medium M199 supplemented with 20% FBS, 1% retinal-derived growth factor, 100 IU mL^{-1} penicillin, 100 μg mL^{-1} streptomycin, and 250 ng mL^{-1} amphotericin B. The medium was changed every 3 days. Retinal-derived growth factor was isolated from bovine retina as described [10]. HUVEC were further characterized by the presence of von Willebrand factor and the absence of smooth muscle α-actin as described previously [11]. EA.hy926 hybrid cells from the human epithelial cell line A549 and HUVEC were a gift from Cora-Jean S. Edgell, University of North Carolina, Chapel Hill and grown as described previously [12]. This cell line has been shown to preserve many features of HUVEC [12–18] and was further characterized in our laboratory by the presence of preproendothelin-1 mRNA and its ability to secrete preproendothelin-1 (data not shown). CHO-K1 ovarian cells from the Chinese hamster (*Cricetulus griseus*) were grown in Ham's F12 medium containing 10% FBS, 100 IU mL^{-1} penicillin, and 100 μg mL^{-1} streptomycin.

Cloning of the NOS-III Adenoviral Transfer Plasmid

The cDNA encoding the constitutive NOS from bovine aortic endothelial cells, *NOS3* (GenBank accession nr M89952) [19], was excised as a 3.7 kb *Eco*RI fragment from the ec NOS plasmid. The NOS-III cDNA was then re-cloned into the *Eco*RI site of the adenoviral transfer plasmid of pAC-CMVpLpA [20]. pAC-CMVpLpA contains an adenovirus type 5 sequence spanning the adenoviral 5′-inverted terminal repeats to np 453, followed by an expression cassette consisting of a CMV promoter/enhancer, pUC19 polylinker, and termination signals of the simian virus 40 3′-untranslated region, followed by a homologous recombination region spanning np 3334 to 6103 of Ad5. To test the correct cloning, the recombinant pAC-CMVpLpA transfer plasmids, designated as NOSIII/pAC-CMV, were transfected into 293 cells. The transfected cells were tested for NOS activity and NOS protein expression by an activity assay and immunoprecipitation.

Development of a Recombinant Replication-Deficient Adenoviral Vector for Endothelial NOS-III

The tested recombinant transfer plasmid NOSIII/pAC-CMV was co-transfected with the circularized adenoviral genome pJM17 into 293 cells, using the calcium phosphate method [21]. The plasmid pJM17 contains the sequence of wild-type adenovirus type 5 plus additional non-viral sequences, which renders pJM17 per se too large to be packaged into infective virion particles. Thus, only homologous recombination *in vivo* between pJM17 and NOSIII/pAC-CMV resulted in recombinant adenoviral genomes carrying the NOS-III expression cassette integrated into a complete, packageable adenoviral genome. The resulting recombinant adenoviral vector was replication-deficient due to a deletion in the E1 region, since the 5′-region was derived from NOSIII/pAC-CMV in which the E1-containing adenoviral sequence between np 453 and 3334 was

missing. Viral plaques appeared between 12 and 24 days after cotransfection. Thereafter, PCR screening for recombinant virus and testing for functional expression of NOS-III was performed as follows. Upon complete lysis of virus-containing cell cultures, standard plaque purification of the total lysate was performed using confluent 293 cell cultures overlaid with low-melting agarose. After 5 to 7 days, single plaques appeared under the agarose overlay and were processed for PCR screening. The plaque material plus agarose was subjected to 3 freeze and thaw cycles, incubated at 37° for 30 min in lysis buffer (16.6 mM ammonium sulfate, 67 mM Tris–HCl, 6.7 mM $MgCl_2$, 5 mM 2-mercaptoethanol, 6.7 mM EDTA, 1.7 mM SDS, 50 μg mL^{-1} proteinase K; pH 6.8) and then inactivated at 85° for 10 min. Finally, DNA was isolated from lysate by standard phenol/chloroform extraction. Using this DNA as a template, recombinant plaques harboring recombinant viruses (Ad5CMVNOSIII) were identified by PCR analysis using the following primer pairs: A, 5′-TCCACGGGCACCTACCACCTC-3′ (NOSIII-codeC) with 5′-GCTCGTTGTCCAGGTGCTTCA-3′ (NOS-antiA); B, 5′-AACTCGACCATCTCTACCGCGACGA-3′ (NOSIII-code) with 5′-CCGGTAAAGGCCAACAGGACA-3′ (NOSIII-antiB); C, NOSIII-code with 5′-TGATAATGAGGGGGTGGAGTTTGT-3′ (Ad5-C3). The three primer pairs resulted in products of sizes 0.8 (A), 0.5 (B), and 1.5 kb (C), respectively. PCR conditions included initial denaturation for 5 min at 94°, followed by 30 cycles comprising 1-min denaturation at 94°, 1-min annealing at 55°, and 2.5 min (plus 10 sec per cycle) of extension at 72°, plus a final extension step of 10 min. PCR-positive clones were subsequently purified by two additional cycles of standard plaque purification and designated as clones Ad5CMVNOSIII. An overview of the construction of the vector is provided in Fig. 1.

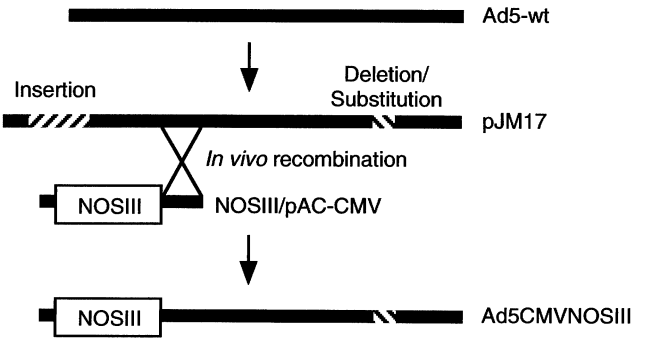

FIG. 1. Construction and cloning of Ad5CMVNOSIII. The schematic map of wild-type Ad5 virus is shown on top. Ad5CMVNOSIII was constructed by *in vivo* recombination of the adenoviral genome plasmid pJM17 with the transfer plasmid NOSIII/pAC-CMV. The plasmid pJM17 contains the sequence of wild-type adenovirus type 5 plus additional non-viral sequences, which renders pJM17 per se too large to be packaged into infective virion particles. Thus, only *in vivo* homologous recombination between pJM17 and NOSIII/pAC-CMV resulted in recombinant adenoviral genomes carrying the NOSIII expression cassette integrated into a complete, packageable adenoviral genome. The resulting recombinant adenoviral vector was replication-deficient due to a deletion in the E1 region, since the 5′-region was derived from NOSIII/pAC-CMV in which the E1-containing adenoviral sequence between np 453 and 334 was missing. Recombination in the indicated region (cross) produces the recombinant NOS-III adenovirus Ad5CMVNOSIII. Black, adenoviral sequences; white box, NOS-III full-length cDNA; hatched, additional plasmid/vector sequences.

Virus Purification and Measurement of Virus Particles

293 cells supported the virus production of the replication-deficient adenovirus because they contain a stable integration of the E1 virus region in their genome. Amplified virus was purified through CsCl gradient centrifugation as described previously [22]. Briefly, after lysis of the infected cells by the cytopathic effect of the adenovirus, Triton® X-100 detergent (final concentration 0.5%) was added to the medium. The suspension was centrifuged (20 min, 4°, 20,000 *g*) and the supernatant precipitated overnight with 0.5 volumes of a 20% solution of polyethyleneglycol 8000 in 2.5 M NaCl and then centrifuged (30 min, 4°, 20,000 *g*). The resulting pellet was resuspended in 4 mL of Tris-buffered saline (10 mM Tris–HCl, 150 mM NaCl, 2 mM $CaCl_2$, 2 mM $MgCl_2$; pH 7.4). CsCl (2 g) was added to the resuspended pellet, incubated for 1 hr at 4°, and then centrifuged (8 min, 4°, 1000 *g*). The supernatant was centrifuged (3 hr, 20°, 353,000 *g*). The virus-containing band was removed and desalted with Tris-buffered saline through NAP-25 columns. The virus content was measured photometrically in the flowthrough fractions (1 $A_{260} = 10^9$ adenovirus particles μL^{-1}).

Infection of Cells

Subconfluent cell cultures were transfected with the Ad5CMVNOSIII vector (1×10^{10} particles per 25 cm^2, if not otherwise stated) in OptiMEM for 4 hr at 37°. Thereafter, the vector was replaced with appropriate culture medium. Infected cells were harvested after 3 days. Cells were washed off with culture medium and pelleted at 260 *g* for 6 min at room temperature. The pellet was washed twice with cold PBS (5 or 10 mL PBS then 260 *g* for 6 min at 4°) and homogenized in NOS buffer (50 mM triethanolamine HCl, 0.5 M EDTA, 7 mM glutathione, 1 μM leupeptin, 1 μM pepstatin, 0.2 mM PMSF; pH 7.5) with the aid of sonifier (Branson Sonifer 250, output 2, duty cycle 50%, 30 sec). To determine the membrane association of NOS-III, the homogenate was centrifuged at 4° for 1 hr with 20,000 *g*. The supernatant was separated and the pellet re-suspended in the NOS buffer. To determine the expression kinetics of NOS-III, subconfluent CHO or EA.hy926 cultures were infected with 1×10^{10} particles per 25 cm^2, and cells were harvested on days 1, 3, 6, 8, and 15 p.i.

Vector Cytotoxicity

Potential cytotoxicity of the vectors was assessed by both morphological analysis and LDH assay using the Cytotox-

icity Detection Kit. EA.hy926 cells were infected with different vectors at 2×10^{10} particles per 9.4 cm^2. Twenty-four hours later, three aliquots of 100 μL medium were removed from each of the infected cultures. LDH assay reaction mix was then added, and LDH activity was determined by measuring the absorbance difference at 490 and 595 nm ($A_{595} - A_{490}$) for each vector. Uninfected cells pretreated with 1% Triton®X-100 served as positive controls, and values are expressed as % of control ± SEM.

Metabolic Labeling and Immunoprecipitation

For the detection of NOS-III expression 3 days after infection of EA.hy926, HUVEC, 293, or CHO cell cultures with Ad5CMVNOSIII vector (1×10^{10} particles per 25 cm^2, if not otherwise stated), metabolic labeling and immunoprecipitation were performed using standard methods [23]. Confluent cell monolayers were washed with PBS, incubated with methionine-free medium (Eagle's minimum essential medium, $Meth^-$ $Glut^-$ substituted with 4 mM glutamine) for 1 hr, and then incubated with 3.7 MBq per 6-cm dish of Trans35label ([^{35}S]methionine) in the same medium for 2–4 hr. Following this pulse, the medium was removed, cells were washed twice with PBS and incubated at 4° for 10 min in lysis buffer (20 mM Tris–HCl, 2 mM $CaCl_2$, 2 mM $MgCl_2$, 150 mM NaCl, 1% Triton®X-100, 1 mM PMSF, 2 μg mL^{-1} leupeptin, 1 μg mL^{-1} pepstatin; pH 8) and then harvested. Immunoprecipitation was performed using affinity-purified polyclonal rabbit anti-human NOS-III antiserum at 4°. After 1 hr of antibody incubation, protein A Sepharose was added and incubated for 1 hr and then pelleted by centrifugation (3 min, 16,000 *g*). Pellets were washed subsequently with 20 mM Tris–HCl (pH 8) containing 2 mM $CaCl_2$, 2 mM $MgCl_2$, 1 mM PMSF, 2 μg mL^{-1} leupeptin, 1 μg mL^{-1} pepstatin, supplemented with either 150 mM NaCl and 0.5% Triton®X-100 (buffer 1), 500 mM NaCl and 0.5% Triton®X-100 (buffer 2), or 150 mM NaCl (buffer 3). Proteins were released from protein A Sepharose beads by denaturation (5 min at 95°) in 2x SDS-PAGE sample buffer (4% SDS, 15% glycerol, 60 mM Tris–HCl, 0.005% bromphenol blue, 100 mM 2-mercaptoethanol; pH 6.8). SDS-PAGE analysis of the ^{35}S-labeled immunoprecipitates was performed under reducing, denaturing conditions in 4–15% SDS-polyacrylamide gradient gels [24]. Fluorography was performed by the standard method using EN^{3}HANCE™ and x-ray films, exposed at −80° for 1–3 days.

Immunocytochemistry

EA.hy926 cells were grown on glass coverslips (14-mm diameter) up to 70% confluency and then infected with Ad5CMVNOS III or Ad5CMVluc as a control vector. Three days after infection, cells were fixed for 10 min with 4% paraformaldehyde in PBS on ice, washed in PBS, and permeabilized for 20 min in PBS containing 0.2% Triton®X-100. Blocking was performed for 20 min in PBS containing 2% normal goat serum, followed by incubation with an affinity-purified polyclonal rabbit anti-human NOS-III antiserum (1 μg mL^{-1} in PBS containing 0.2% BSA) for 1 hr at room temperature. After a 3 × 5 min washing in PBS, cells were incubated with secondary antibody FITC-conjugated goat anti-rabbit immunoglobulin G antiserum (1:100 diluted in PBS, 0.2% BSA) for 1 hr, washed again 3 × 5 min in PBS, counterstained with propidium iodide, and mounted with Vectashield Mounting Medium. Immunofluorescence was detected on an Aristoplan fluorescence microscope.

Cell Proliferation Assay

The effects of the Ad5CMVNOSIII adenovirus on cell proliferation of EA.hy926 cultures were investigated by means of a conventional cell proliferation assay. Cultures of EA.hy926 cells were plated at low, mid, and high density one day before transfection (day-1) and contained approximately 5,000, 50,000, and 500,000 cells per 9.4 cm^2 well, respectively. On day 0, EA.hy926 cultures were transfected with Ad5CMVNOSIII or Ad5CMVluc vector in OptiMEM (1×10^{10} particles of either vector per 9.4 cm^2) or in OptiMEM alone as controls, for 4 hr at 37°. Thereafter, vectors were removed and EA.hy926 cells were maintained in full medium containing 10% serum. To obtain cell counts, cells were trypsinized on day 3 and suspended in 0.1% trypan blue dye. Single cells excluding trypan blue were counted using a haemocytometer. The percentage difference in cell numbers on day 3 over untransfected controls was calculated and expressed as mean ± SEM of *n* separate experiments.

NOS Activity Assay

NOS activity was measured by the conversion of L-arginine to L-citrulline [25]. Unless otherwise indicated, 10 μL cell homogenate was incubated for 30 min at 37° in a total volume of 0.1 mL of 50 mM triethanolamine–HCl (pH 7.0) buffer containing 50 nM CaM, 0.5 mM $CaCl_2$, 5 μM FAD, 10 μM FMN, 250 μM 3-[(3-cholamidopropyl)dimethylammonio]-2-hydroxy-1-propanesulfonate, 5 μM (1′*R*,2′*S*,6*R*)-5,6,7,8-tetrahydrobiopterin, 1 mM NADPH, 7 mM glutathione, and 10 μM L-arginine including 5.55 kBq L-[2,3,4,5-^{3}H]-arginine. The reaction was stopped with 0.9 mL of cold stop buffer (20 mM sodium acetate, 2 mM EDTA; pH 5.5). Citrulline was extracted by chromatography on a 0.8-mL cation exchange column (Dowex AG 50 W-X8 resin, Na^+ form) pre-equilibrated with stop buffer. The combined column flowthrough (1 mL) and a water eluate (2 mL) were measured for ^{3}H radioactivity in 10 mL Rotiszint eco plus by liquid scintillation counting.

Protein Determination

Protein concentrations were determined according to Bradford in a microplate format assay using BSA as a standard [26]. All measurements were performed in triplicate.

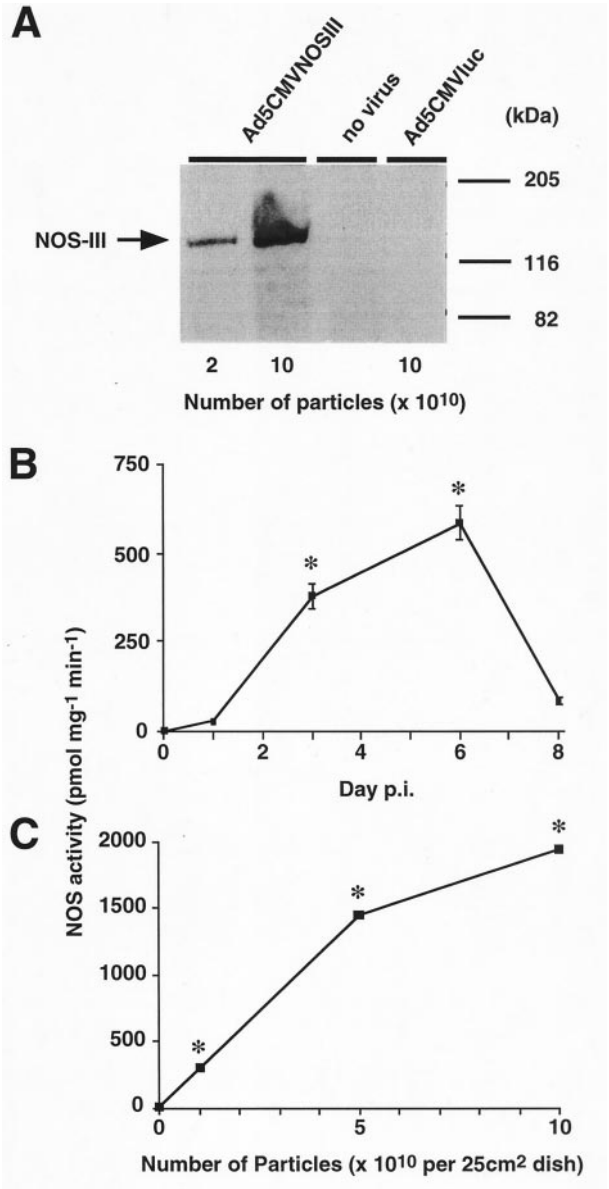

FIG. 2. Virological characterization of the Ad5CMVNOSIII vector. (A) Metabolic labeling and immunoprecipitation of NOS. CHO cells were either infected with different multiplicities of infection (2×10^{10} or 1×10^{11} particles per dish) of Ad5CMVNOSIII or not infected. After 3 days, the cells were labeled with ^{35}S and NOS-III was immunoprecipitated as described. The position of molecular mass standards is indicated on the right, while the arrow on the left shows the position of the NOS-III immunoreactive protein band with the apparent molecular mass of 130 kDa. The dose-dependent expression of NOS-III antigen is shown in lane 1 (2×10^{10} particles per 25 cm^2) and lane 2 (1×10^{11} particles per 25 cm^2); lanes 3 and 4 demonstrate the absence of endogenous NOS-III antigen in uninfected (lane 3) or in Ad5CMVluc-infected control cells (lane 4). Results are representative of 10 independent experiments with similar results. (B) Kinetics of the NOS production in CHO cells. To determine the expression kinetics of NOS-III, subconfluent CHO cultures were infected with 1×10^{10} particles per 25 cm^2 and cells harvested on days 1, 3, 6, and 8. NOS activity was then measured with 30 μL cell lysate and expressed as pmol citrulline formed per mg protein per min. Values represent the means ± SEM of triplicate determinations of pooled material from 2 dishes. Control cells had no detectable

Kinetic Analysis

NOS activity is reported as pmol citrulline formed per mg of protein per min (specific activity), total product accumulation in pmol of citrulline, or as % of control. To determine K_m, K_a or V_{max} values, the standard assay time was 30 min up to which product formation was linear. Calculations were done for NADPH and L-arginine by a one-site binding hyperbolic equation [specific activity = $(V_{max} \cdot c)/(K_m + c)$] and for H_4Bip by a sigmoidal concentration–response equation [specific activity = $V_0 + (V_{max} - V_0)/(1 + 10^{\log EC\ 50\ -\ log\ c})$] with the aid of the Prism 2.0 software (GraphPad), where V_{max} means the maximal activity, V_0 the basal activity in the absence of H_4Bip, and c is the used concentration of NADPH, L-arginine, or H_4Bip.

Statistics

The results shown represent mean values ± SEM of n experiments. For comparisons, we used one-way analysis of variance (ANOVA) followed by Dunnett's Multiple Comparison Test or Bonferroni's Multiple Comparison Test. A P value < 0.05 was considered to be significant.

RESULTS

Construction and Cloning of Ad5CMVNOSIII

Despite optimized transfection and cell culture conditions, the rate at which recombinant viruses formed by homologous recombination (Fig. 1) was very low, far lower than in a series of 24 other transgenes cloned in the same vector system. Amongst six recombinant viruses from a series of cotransfection experiments in which integration of NOS-III sequences was detected by PCR, only one clone (Ad5CMVNOSIII #96/14) was functionally active, expressing endothelial NOS-III after infection of HUVEC or CHO cells.

Virus Characterization

We evaluated the efficacy of Ad5CMVNOSIII gene transfer first in CHO cells by measuring levels of NOS-III immunoreactive protein and enzymatic NOS activity. NOS-III immunoreactive protein was readily detectable in infected cells, while non-infected cells were negative (Fig. 2A). The level of activity was up to 1350 pmol mg^{-1} min^{-1} with considerable variability, depending on the prepara-

FIG. 2. (continued) NOS activity. *$P < 0.001$ vs control. (C) Dose–response of adenoviral gene transfer of NOS-III to CHO cells. CHO cells were infected with different amounts of virus (1×10^{10}, 5×10^{10}, or 10×10^{10} particles per 25 cm^2 dish) or not infected. Cells were harvested on days 3 p.i. and NOS activity was then measured with 30 μL cell lysate (see above). Control cells had no detectable NOS activity. *$P < 0.001$ vs control and all other doses. Results are representative of 3 independent experiments with similar results.

tion. To further characterize the ability of the non-replicating adenoviral vector to infect cells, we measured NOS activity in cell homogenates after infection with different multiplicities of infection and investigated the time–course of NOS expression. NOS activity peaked at day 6 p.i., was still detected at day 8 p.i., but then declined (Fig. 2B). To investigate the relationship between NOS-III protein expression and NOS activity, we evaluated the effects of different infectious titers on these parameters. Both protein expression levels and specific NOS activity correlated with increasing titers of viral infection up to 1×10^{11} particles (Fig. 2, A and C). Further increasing the multiplicity of infection resulted in cytotoxic effects (data not shown).

Enzyme Domains and Kinetics

To characterize the expressed NOS and to ensure its proper expression and functionality, including the very C-terminal NADPH binding site, we chose the CHO and 293 cell lines as a model system and later verified these results on EA.hy926 endothelial cells as model systems for later gene transfer. In permissive 293 cells, we reached NOS activities up to 1375 $pmol^{-1}$ mg^{-1} min^{-1}, which were similar to those observed for CHO cells. All known NOS binding sites were characterized, beginning from the N-terminus (L-arginine, H_4Bip) via Ca^{2+}/CaM, FMN, and FAD to the very C-terminal, and thus conceivably most critical, NADPH binding site. We also examined the time–course of citrulline formation and enzyme stability.

The kinetics of the citrulline accumulation in both cell lines revealed that the reaction was linear with time for up to 20–30 min; afterwards, a small decline in activity was observed (Fig. 3A). To examine the correct function of the N-terminal oxygenase domain, we determined the dependence on L-arginine as a test for the oxygenase domain function of NOS-III. The concentration–response curves showed that citrulline production of the adenovirally transferred NOS-III was strictly dependent on L-arginine, with a K_m value for L-arginine of 13.8 ± 0.4 μM for 293 cells and 12.3 ± 7.9 μM for CHO cells (Fig. 3B). We next investigated the concentration–response curve to H_4Bip, a known oxygenase domain marker and NOS activator, in CHO and 293 cell homogenates. NOS-III from these 293 adenovirus-infected cells was clearly dependent on H_4Bip, with a K_a of 0.14 ± 0.02 μM for 293 cells and 0.10 ± 0.02 μM for CHO cells. Maximal activity was observed in the presence of 1 μM H_4Bip (Fig. 3C). Basal activity was possibly due to partial saturation with cell-derived pterin.

To investigate the Ca^{2+} dependence of CaM binding to NOS-III, we measured citrulline formation in the absence or presence of Ca^{2+}. No activity in either CHO or 293 cells was observed when NOS-III was incubated in Ca^{2+}-free buffer containing 5 mM EGTA (Fig. 4A). This experiment also demonstrated the absence of Ca^{2+}-independent NOS-II in these cells upon infection with Ad5CMVNOSIII. In contrast, NOS activity in 293 and CHO cells was reduced only slightly when no CaM was added, presumably due to the presence of sufficient endogenous CaM in these cell lysates (Fig. 4B).

We then examined the dependence of NOS activity on FMN and FAD. Similar to native enzyme, which quantitatively binds flavins, adenovirally transferred NOS activity was not affected in the absence of exogenous FAD (Fig. 5A). In the case of FMN, there was only a small reduction in 293 and CHO cells when this cofactor was omitted (Fig. 5B). This indicates nearly complete saturation of NOS-III with cell-derived flavins. Next, we examined the dependence on NADPH as a functional test for the very C-terminal of the reductase domain of NOS-III. The concentration–response curves with NADPH showed that citrulline production of the adenoviral-transferred NOS-III was strictly dependent on NADPH, with a K_m value of 271.4 ± 228.8 μM NADPH for 293 cells and 3.7 ± 13.1 μM for CHO cells (Fig. 5C). The apparent differences are probably due to low molecular weight components interfering with NADPH binding or consuming NADPH in the crude cell homogenates [27].

NOS Expression in Vascular Cells

Because of the possible relevance of Ad5CMVNOSIII vectors for vascular gene therapy, we next characterized NOS-III gene transfer in vascular cells. In primary human vascular endothelial cells, NOS-III immunoreactive protein could be easily detected by ^{35}S metabolic labeling and immunoprecipitation at day 3 p.i. The expressed NOS-III had the expected molecular mass of 130 kDa as determined by SDS-PAGE after immunoprecipitation. Moreover, expression of NOS-III immunoreactive protein was dose-dependent with respect to Ad5CMVNOSIII, reaching a maximum with 1×10^{11} particles (Fig. 6A). To determine whether the expressed NOS-III was membrane-associated, we separated the cell homogenate into supernatant and pellet and measured the distribution of NOS activity. About 85% of total activity was localized in the pellet. Additionally, the specific activity in the pellet fraction was 7 times higher than in the supernatant. In EA.hy926 cells, NOS activities ranged from 0.6–688 pmol mg^{-1} min^{-1}, and the expressed NOS-III could be easily detected in immunoprecipitates (Fig. 6B). The kinetics of the NOS activity in infected cells is shown in Fig. 7A. The highest level of activity was found on day 3 p.i., decreased on day 6 and 8, and was no longer detectable by day 15 p.i. NOS-III from the EA.hy926 cells showed a nearly absolute requirement for Ca^{2+}, and citrulline formation was significantly reduced in the absence of added flavins or H_4Bip (Fig. 7B). Concentration–response curves for NADPH showed that citrulline production of the adenoviral-transferred NOS-III was strictly dependent on NADPH, with a K_m of 53.3 ± 12.3 μM (Fig. 7C). Maximal activity was achieved in the presence of 300 μM NADPH.

In order to further characterize the predominantly particulate cellular localization of NOS-III after transfection in EA.hy926 endothelial cells, we performed immunocyto-

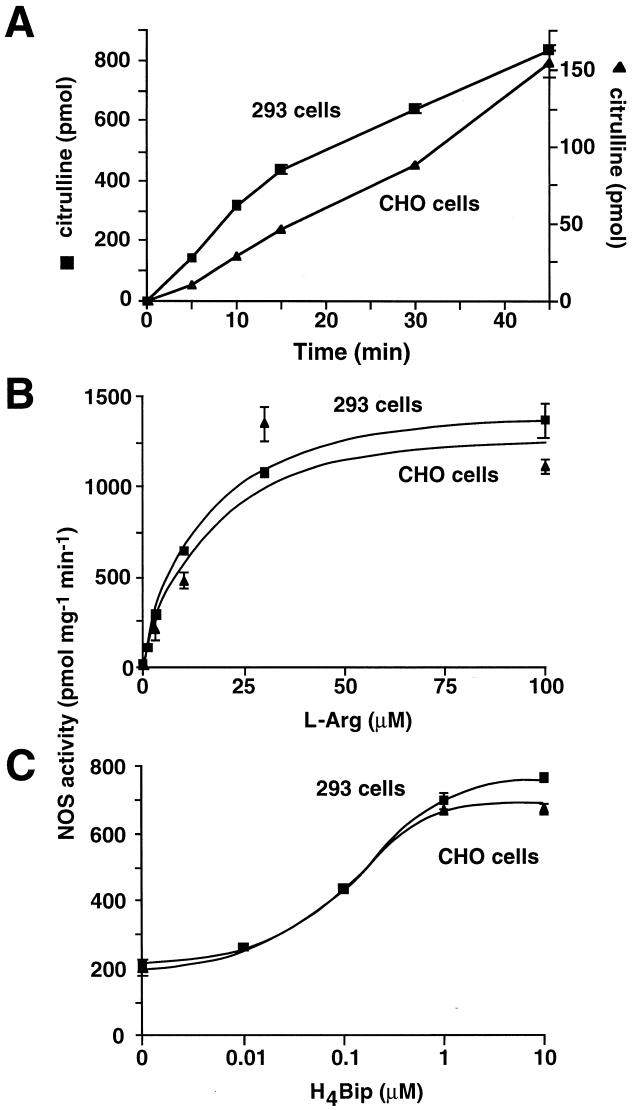

FIG. 3. Biochemical characterization of the oxygenase domain. (A) Kinetics of citrulline production by recombinant NOS-III in 293 (■) and CHO (▲) cell homogenate (10 μL). NOS activity was assayed for different time points (0–45 min) and is expressed as absolute pmol citrulline formed. Symbols represent the means ± SEM of N = 3 experiments. (B) Determination of the K_m value for L-arginine of NOS-III from 293 (■) and CHO (▲) cells. Ten μL cell homogenate from infected cells was assayed for NOS activity with increasing concentrations of L-arginine. Symbols represent the means ± SEM of N = 3 experiments. Lines are fitted to a hyperbolic Michaelis–Menten function. (C) Determination of the K_a for H_4Bip of NOS-III from 293 (■) and CHO (▲) cells. Ten μL cell homogenate from infected cells was assayed for NOS activity in the presence of increasing concentrations of H_4Bip. Symbols represent the means ± SEM of N = 3 experiments. Lines are fitted to a sigmoidal concentration–response function.

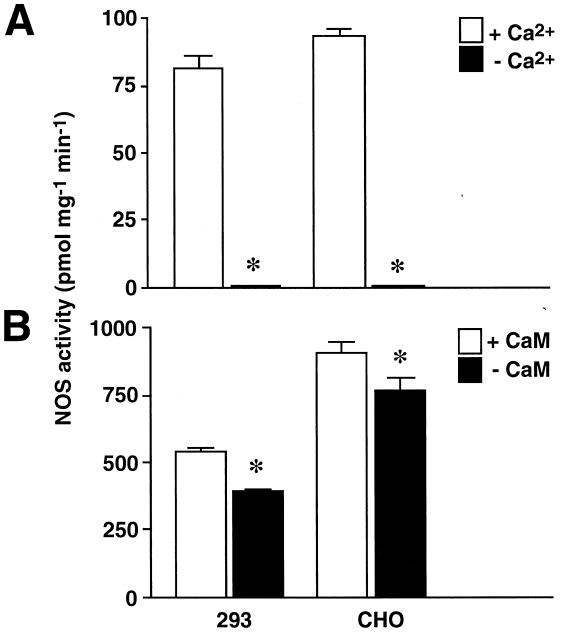

FIG. 4. Ca^{2+}/CaM-dependence of recombinant NOS-III. (A) Ca^{2+} dependence of citrulline formation. Ten μL cell homogenate from infected 293 and CHO cells was assayed for NOS activity either in the presence (open bars) or absence of Ca^{2+} (closed bars). Ca^{2+}-free conditions were ensured by adding 5 mM ethyleneglycole tetraacetic acid to chelate all Ca^{2+} from the cell homogenate. Values represent the means ± SEM of N = 3 experiments. *P < 0.0001 vs control. (B) Dependence on CaM for citrulline formation. Ten μL cell homogenate from infected 293 and CHO cells was assayed for NOS activity either in the presence (open bars) or absence of CaM (closed bars). Values represent the means ± SEM of N = 3 experiments. *P < 0.01 vs control.

chemistry using a commercial NOS-III antibody. Only in cells infected with Ad5CMVNOSIII was a granule NOS-III immunoreactive staining of cytoplasm and cell membrane seen, whereas no staining was observed in control cells infected with Ad5CMVluc (Fig. 8). This observation underscores the correct expression and subcellular localization of adenovirally transferred NOS-III in endothelial cells. Figure 8 shows also the high efficiency of the gene transfer to EA.hy926 cell. In the presence of 1×10^{10} Ad5CMVNOSIII particles per 25 cm^2, about 95% of the cells were infected as assessed by immunostaining and quantitation of NOS-III immunoreactive and negative cells.

Besides acute vasorelaxation, the antiproliferative effects of NO may also be relevant *in vivo*. To investigate the effects of overexpressed NOS-III on endothelial cells as possible relevant target cells, we used a conventional cell proliferation assay. Infection of EA.hy926 cells resulted in a significant inhibition of cell proliferation when compared to uninfected or mock-infected (luciferase-expressing vector). This effect was independent of the plated cell density (Fig. 9). The decrease in cell proliferation with the NOS-III vector may, however, be due to the cytotoxic potential of NO. Confounding effects due to cytotoxicity of the vector itself were mitigated by counting viable cells only. The percentage of dead cells was always below 10%, and no significant differences in the fraction of trypan blue positive cells were observed between the different treatment groups. Furthermore, none of the vectors used was cytotoxic when assessed by morphological analysis and LDH release assay

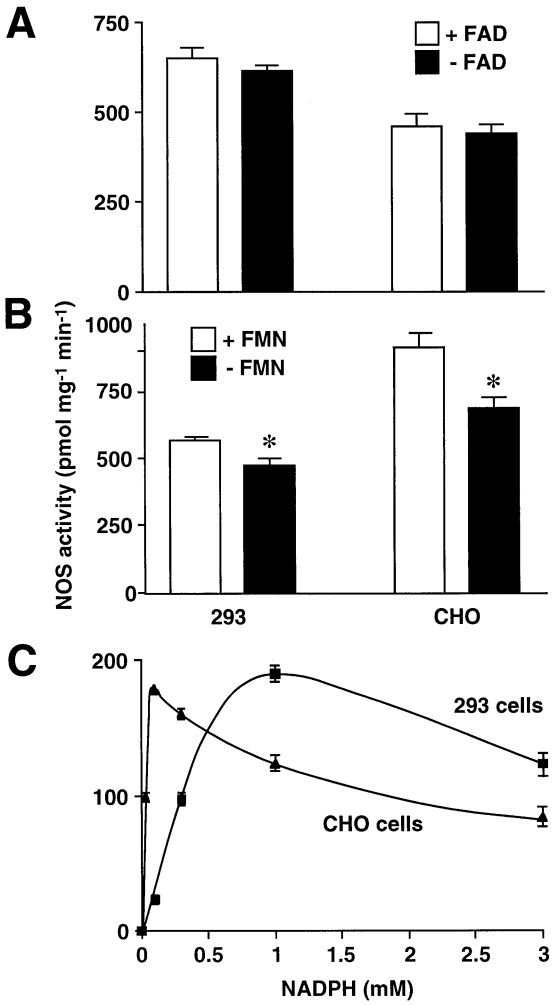

FIG. 5. Biochemical characterization of the reductase domain. (A) Dependence on FAD for citrulline formation. Ten μL cell homogenate from infected 293 and CHO cells was assayed for NOS activity either in the presence (open bars) or absence of FAD (closed bars). Values represent the means ± SEM of N = 3 experiments. (B) Dependence on FMN for citrulline formation. Ten μL cell homogenate from infected 293 and CHO cells was assayed for NOS activity either in the presence (open bars) or absence of FMN (closed bars). Values represent the means ± SEM of N = 3 experiments. *$P < 0.005$ vs control. (C) Determination of the K_m for NADPH of NOS-III from 293 (■) and CHO (▲) cells. Ten μL cell homogenate from infected cells was assayed for NOS activity in the presence of increasing concentrations of NADPH. Symbols represent the means ± SEM of N = 3 experiments.

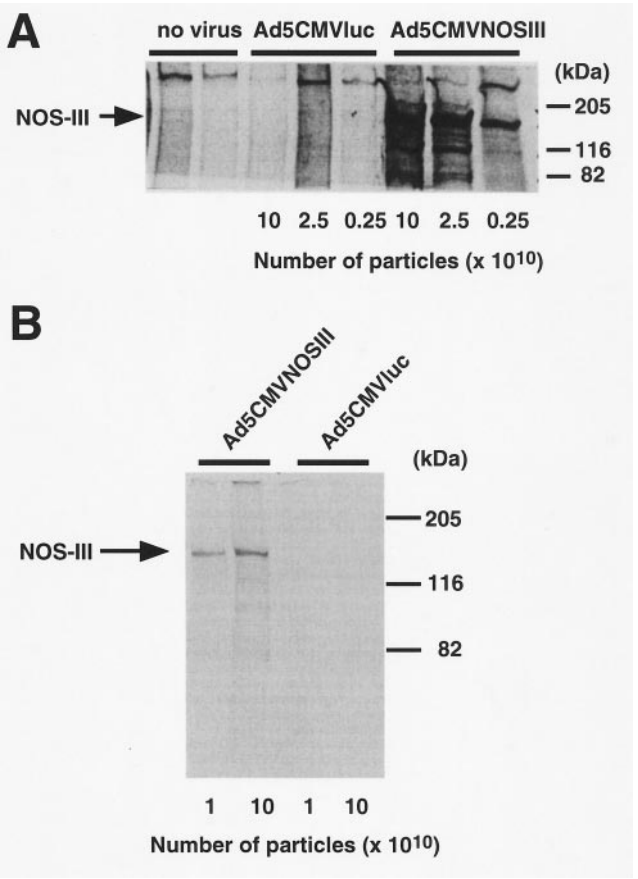

FIG. 6. Metabolic labeling and immunoprecipitation of NOS-III in endothelial cells. (A) HUVEC were infected with different multiplicities of infection (2.5×10^9 or 2.5×10^{10} or 1×10^{11} particles per dish) of Ad5CMVNOSIII, Ad5CMVluc (control), or not infected. After 3 days, the cells were labeled with ^{35}S and the NOS-III immunoreactive protein precipitated as described. The position of molecular mass standards is indicated on the right, while the arrow on the left shows the position of the NOS-III protein band with the apparent molecular mass of 130 kDa. Lanes 1–5 demonstrate the absence of endogenous NOS-III antigen in uninfected (lanes 1, 2) or in Ad5CMVluc-infected control cells (lanes 3–5). The dose-dependent expression of NOS-III antigen is shown in lane 6 (1×10^{11} particles per 25 cm^2), lane 7 (2.5×10^{10} particles per 25 cm^2), and lane 8 (2.5×10^9 particles per 25 cm^2). (B) EA.hy926 cells were infected with different multiplicites of infection (1×10^{10} or 1×10^{11} particles per dish) of Ad5CMVNOSIII or Ad5CMVluc as control. After 3 days, the cells were labeled with ^{35}S and the NOS-III immunoreactive protein precipitated as described. The position of molecular mass standards is indicated on the right, while the arrow on the left shows the position of the NOS-III protein band with the apparent molecular mass of 130 kDa. The dose-dependent expression of NOS-III antigen is shown in lane 1 (1×10^{10} particles per 25 cm^2) and lane 2 (1×10^{11} particles per 25 cm^2). Lanes 3 and 4 demonstrate the absence of endogenous NOS-III antigen in Ad5CMVluc-infected control cells (lane 3, 1×10^{10} particles per 25 cm^2 and lane 4, 1×10^{11} particles per 25 cm^2). Results are representative of 13 independent experiments with similar results.

(Ad5CMVNOSIII, 3.3 ± 0.4% of control; Ad5CMVluc, 3.0 ± 0.0%; uninfected cells, 3.1 ± 0.3%; differences not significant). Vectors containing luciferase constructs had no obvious effect on cell proliferation either.

DISCUSSION

Virus-mediated NOS-III gene transfer has become a frequently used method to modulate vascular functions in different organs *in vivo*. However, in most of these studies either the expressed NOS-III was not biochemically characterized or the primary target, vascular endothelium, was not examined [2, 28–34]. During the production of a highly complex protein such as recombinant NOS-III, it is mandatory to characterize any such vector not only by molec-

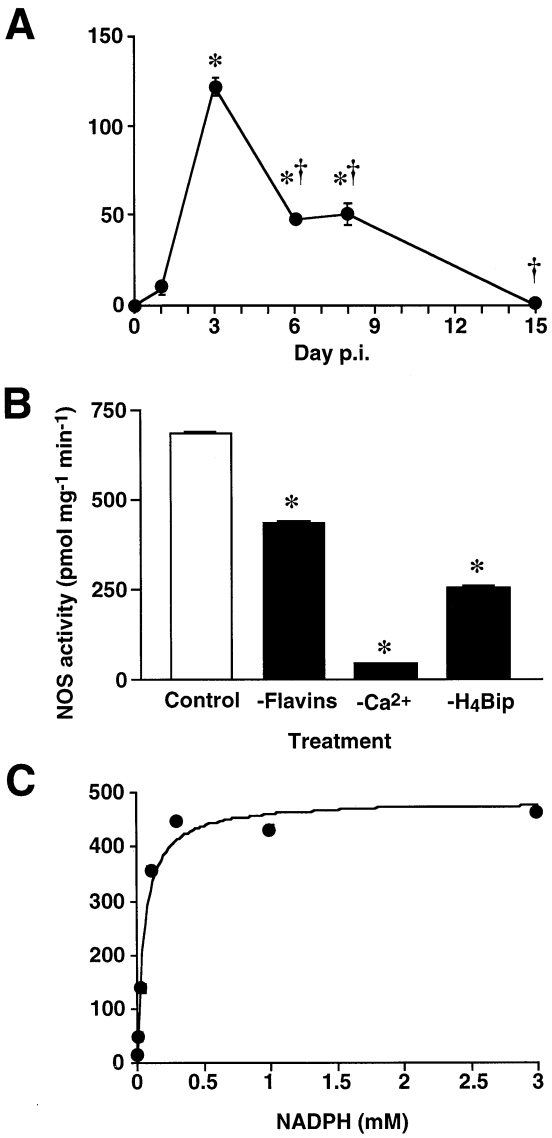

FIG. 7. Characterization of NOS from infected endothelial cells. (A) Kinetics of NOS production in EA.hy926 cells. To determine the expression kinetics of NOS-III, subconfluent EA.hy926 cultures were infected with 1×10^{10} particles per 25 cm^2 and cells harvested on days 1, 3, 6, 8, and 15. NOS activity was then measured with 40 μL cell lysate and expressed as pmol citrulline formed per mg protein per min. Values represent the means ± SEM of triplicate determinations of pooled material from 2 dishes. Control cells had no detectable NOS activity. *$P < 0.001$ vs uninfected control, †$P < 0.001$ vs infected cell cultures on day 3 p.i.. (B) Co-factor dependence of citrulline formation. Five μL cell homogenate from infected cells was assayed for NOS activity as described (control) or without flavins (FAD and FMN), H_4Bip, or Ca^{2+}. Ca^{2+}-free conditions were ensured by adding 5 mM ethyleneglycole tetraacetic acid to chelate all Ca^{2+} from the cell homogenate. Values represent the means ± SEM of N = 3 experiments. *$P < 0.01$ vs control. (C) Determination of the K_m for NADPH of NOS-III from EA.hy926 cells. Ten μL cell homogenate from infected cells was assayed for NOS activity in the presence of increasing concentrations of NADPH. Symbols represent the means ± SEM of N = 3 experiments. Lines are fitted to a hyperbolic Michaelis–Menten function.

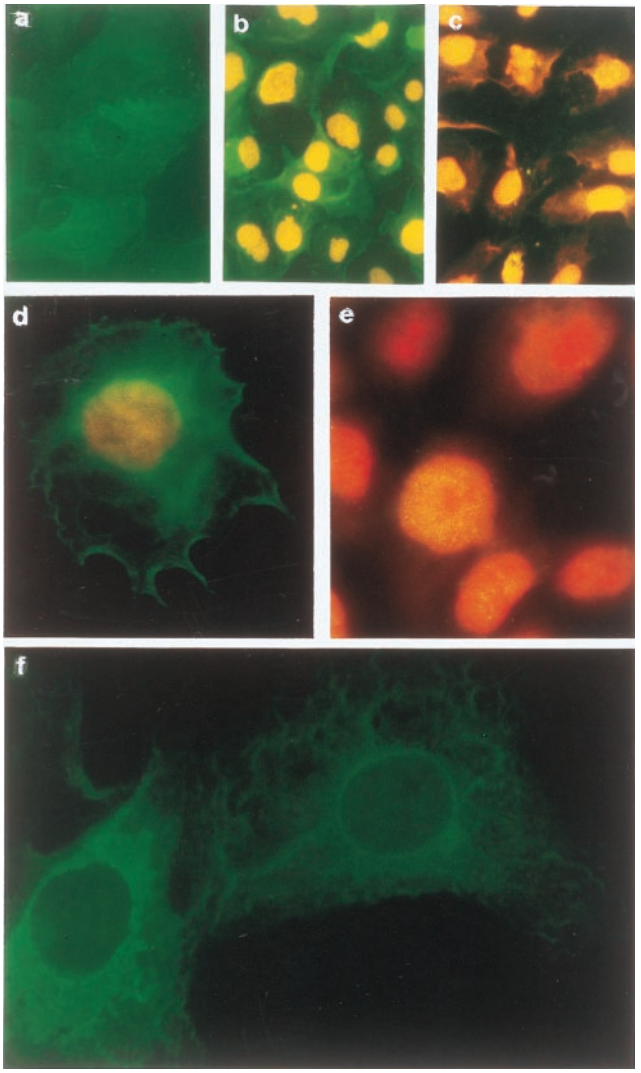

FIG. 8. Immunostaining of EA.hy926 cells following Ad5CMVNOSIII-mediated gene transfer of NOS-III. EA.hy926 cells were infected with either Ad5CMVNOSIII (a, b, d, f) or Ad5CMVluc as a control (c, e), immunostained with a primary anti-NOS-III antibody, secondary FITC-conjugated antibody, and then counterstained with propidium iodide, as described. (a) Fluorescent immunocytochemistry with NOS-III antibody (green); (b) double-fluorescence labeling with NOS-III antibody (green) and propidium iodide (yellow); (c) double-fluorescence labeling with NOS-III antibody and propidium iodide (negative control); (d) double-fluorescence labeling with NOS-III antibody and propidium iodide (higher magnification); (e) double-fluorescence labeling with NOS-III antibody and propidium iodide (negative control) (higher magnification); (f) fluorescent immunocytochemistry with NOS-III antibody (higher magnification).

ular and virological methods, but also by biochemical evaluation of its precise enzymatic functionality. This will also help to exclude possible vector artifacts, i.e. viruses that contain the desired transgene but do not express functionally active NOS-III. We have previously never encountered this type of artifact when producing vectors for a total of two dozen different transgenes. Therefore, the specific transgene product of NOS-III, i.e. NO, appears to

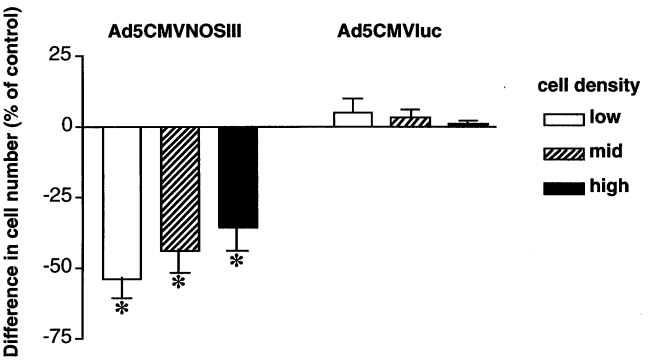

FIG. 9. Influence of Ad5CMVNOSIII on cell proliferation. Cells were infected with Ad5CMVNOSIII and cell proliferation was measured as described under Methods. Results are shown in percent difference of the cell count after infection versus uninfected controls, expressed as means ± SEM of N = 3–7 separate experiments. Low- (open bars), mid- (hatched bars), and high-density (closed bars) cultures of EA.hy926 cells were plated on day −1. On day 0, cultures were infected with Ad5CMVNOSIII or Ad5CMVluc and on day 3 p.i. final cell numbers were obtained. *$P < 0.01$ indicates significant difference of infected cell count versus uninfected control and Ad5CMVluc-infected cultures.

interfere with the cloning procedure, involving multiple steps of amplifying recombinant virus in permissive 293 cells. In fact, inhibition of adenoviral replication by NO has been described previously [35–37]. If this is so, NOS-III would be the first example of a transgene which is difficult to clone and propagate in a viral vector due to autoinhibition of the transgene itself. Further studies investigating and attempting to overcome this problem are under way. One approach is to use an endothelial-or smooth muscle cell-specific promotor which is not active in the 293 cells used for cloning, but in the desired target cells. This would also answer the question as to whether NO interferes with the cloning procedure or not.

We successfully overexpressed NOS-III using a recombinant adenoviral vector. In metabolic labeling and immunoprecipitation studies, NOS-III antigen was evident in HUVEC, EA.hy926, and 293 cells using low virus doses, whilst higher doses were required to detect its expression in CHO cells. As the latter are derived from Chinese hamster ovary, it is most likely that this is a reflection of species difference, in that binding of the human adenovirus penton fibers occurs preferentially to human adenovirus receptors. This is further supported by our observation that luciferase activity is consistently lower in Ad5CMVluc-transfected rat primary vascular smooth muscle cells and CHO cells than in EA.hy926 cells or human primary vascular smooth muscle cells (data not shown).

As expected, endogenous expression of NOS-III antigen was absent from CHO and 293 cells [38, 39]. Basal expression of immunoreactive NOS-III antigen was below our detection limit in membrane preparations of untransfected EA.hy926 cells or in primary cultures of HUVEC. In accordance with this, NOS-III activity was also not detected in untransfected HUVEC or EA.hy926 cells. In a recent study, we found that the basal level of NOS-III expression in HUVEC prepared according to our identical protocol was near the detection limit, but could be upregulated*. Endothelial genes, including NOS-III, may be affected by the cell culture conditions as compared to the intact blood vessel. Some factors that may regulate NOS-III gene expression include shear stress, tumor necrosis factor-α, or hypoxia, which could also be important for cell culture of endothelial cells [18, 40]. Furthermore, our immunoprecipitation assay used to detect NOS apparently lacked sensitivity. For EA.hy926 cells, the absence of basal NOS activity was reported previously [41]. However, arginine to citrulline conversion activity was elevated significantly in Ad5CMVNOSIII-transfected EA.hy926 cells and was confirmed as NOS-III activity by its absolute dependence on free Ca^{2+}. The fact that NOS activity in crude cell lysates was independent of added calmodulin indicates that in intact cells as well the enzyme can be maximally activated by calmodulin, depending on elevated free Ca^{2+}. The activity of recombinant NOS-III reached its peak at day 3 following transfection, but was no longer detectable after day 15. Similarly, adenovirus-mediated transfer of NOS-III into rat lungs was associated with maximal arginine conversion 4 days after NOS-III transduction [42]. Our *in vitro* studies indicate that the termination of vector-mediated NOS-III overexpression occurs after two weeks, despite the absence of a specific anti-vector immune response that occurs regularly *in vivo*.

The biochemical characterization of Ad5CMVNOSIII-transfected enzyme revealed that the recombinant NOS-III had the same properties as native enzyme. The enzyme was mostly located in the particulate fraction, suggesting correct acylation and caveolin interaction. This finding was also confirmed by immunocytochemistry. The specific activities of the protein in homogenates were high when compared to published values of other adenovirus-transfected cells and indicate sufficient expression in order to observe biological or therapeutic effects [31, 32]. Moreover our virus stock was specifically selected for high transfection efficiency and enzyme activity. The virus doses used were adequate to infect nearly all cells in the absence of cytotoxic effects. The expressed protein appeared reasonably stable for up to 20 min. All biochemical and enzyme kinetic data were in good agreement with published values for L-arginine, Ca^{2+}, H_4Bip, and NADPH binding by native NOS-III. An intriguing observation in the present study was that Ad5CMVNOSIII transfection of EA.hy926 led to a reduction in cell proliferation. We have previously shown that adenoviral vectors allow specific modulation of intracellular signaling pathways, provided that the vector dose is appropriate for the target cell or tissue under investigation [43, 44]. In addition to the basic characterization of vectors intended for use in gene therapy protocols, we have demonstrated physiological regulation of our potentially

* Butt E, Smolenski A, Melichar V, Kotsonis P, Bernhardt M, Lohmann SM and Schmidt HHHW, unpublished results.

therapeutic transgene product, which is particularly important for transgenes with highly complex biological functions such as NOS-III. The kinetics of transgene expression in the intended target cells has also been characterized in detail, which is essential for a realistic assessment of what can possibly be achieved when applying the gene therapy vector *in vivo*. Short-term expression could be sufficient for the prevention of restenosis, whereas very stable expression would be necessary to potentially influence long-term processes such as atherosclerosis progression in certain vascular areas. The latter goal appears to be beyond what can be achieved by using the vector characterized here, whereas the vector could be useful for restenosis prevention and other applications. In summary, our NOS-III adenovector provides a valuable and well-characterized tool for further *in vivo* studies on the gene therapy of vascular disease states.

This work was supported by the Deutsche Forschungsgemeinschaft through SFB 355/C7 (W. P. and H. H. H. W. S.) and through a Heisenberg fellowship to W. P. (378/2-1 and 378/2-2). We thank Birgit Wagner and Petra Thalheimer for excellent technical assistance.

References

1. Schmidt HHHW and Walter U, NO at work. *Cell* **78:** 919–925, 1994.
2. von der Leyen HE, Gibbons GH, Morishita R, Lewis NP, Zhang L, Nakajima M, Kaneda Y, Cooke JP and Dzau VJ, Gene therapy inhibiting neointimal lesions: *In vivo* transfer of endothelial cell nitric oxide synthase gene. *Proc Natl Acad Sci USA* **92:** 1137–1141, 1995.
3. Ignarro LJ, Buga GM, Wood KS, Byrns RE and Chaudhuri G, Endothelium-derived relaxing factor produced and released from artery and vein is nitric oxide. *Proc Natl Acad Sci USA* **84:** 9265–9269, 1987.
4. Huang PL, Huang Z, Mashimo H, Bloch KD, Moskowitz MA, Bevan JA and Fishman MC, Hypertension in mice lacking the gene for endothelial nitric oxide synthase. *Nature* **377:** 239–242, 1995.
5. Shesely EG, Maeda N, Kim H-S, Desai KM, Krege JH, Laubach VE, Sherman PA, Sessa WC and Smithies O, Elevated blood pressures in mice lacking endothelial nitric oxide synthase. *Proc Natl Acad Sci USA* **93:** 13176–13181, 1996.
6. Miyamoto Y, Saito Y, Kajiyama N, Yoshimura M, Shimasaki Y, Nakayama M, Kamitani S, Harada M, Ishikawa M, Kuwahara K, Ogawa E, Hamanaka I, Takahashi N, Kaneshige T, Teraoka H, Akamizu T, Azuma N, Yoshimasa Y, Yoshimasa T, Itoh H, Masuda I, Yasue H and Nakao K, Endothelial nitric oxide synthase gene is positively associated with essential hypertension. *Hypertension* **32:** 2–8, 1998.
7. Villanueva MET, Zaher FM, Svinarich DM and Konduri GG, Decreased gene expression of endothelial nitric oxide synthase in newborns with persistent pulmonary hypertension. *Pediatr Res* **44:** 338–343, 1998.
8. Arngrímsson R, Hayward C, Nadaud S, Baldursdóttir Á, Walker JJ, Liston WA, Bjarnadóttir RI, Brock DJH, Geirsson RT, Connor JM and Soubrier F, Evidence for a familial pregnancy-induced hypertension locus in the eNOS-gene region. *Am J Hum Genet* **61:** 354–362, 1997.
9. Poller W, Schneider-Rasp S, Liebert U, Merklein F, Thalheimer P, Haack A, Schwab R, Schmitt C and Brackmann H-H, Stabilization of transgene expression by incorporation of E3 region genes into adenoviral factor IX vector and by transient anti-CD4 treatment of the host. *Gene Ther* **3:** 521–530, 1996.
10. Draijer R, vaan Drager AB, Nolte C, de Jonge HR, Walter U and van Hinsbergh VWM, Expression of cGMP-dependent protein kinase I and phosphorylation of its substrate, vasodilator-stimulated phosphoprotein, in human endothelial cells of different origin. *Circ Res* **77:** 897–905, 1995.
11. Yu JCM and Davenport AP, Secretion of endothelin-1 and endothelin-3 by cultured human vascular smooth muscle cells. *Br J Pharmacol* **114:** 551–557, 1995.
12. Edgell CJS, McDonald CC and Graham JB, Permanent cell line expressing human factor VIII-related antigen established by hybridization. *Proc Natl Acad Sci USA* **80:** 3734–3740, 1983.
13. Newman PJ, Berndt MC, Gorski J, White GC, Lyman S, Paddock C and Muller WA, PECAM-1 (CD31) cloning and relation to adhesion molecules of the immunoglobulin gene superfamiliy. *Science* **247:** 1219–1222, 1990.
14. Simmons DL, Satterwaite AB, Tenen DG and Seed B, Molecular cloning of a cDNA encoding CD34, a sialomucin of human hematopoietic stem cell. *J Immunol* **148:** 267–271, 1992.
15. Bussolino F, Wang JM, Defilippi P, Turrini P, Sanavio F, Edgell C-JS, Aglietta M, Arese P and Mantovani A, Granulocyte- and granulocyte-macrophage-colony stimulating factors induce human endothelial cells to migrate and proliferate. *Nature* **337:** 471–473, 1989.
16. Johnston GI, Cook RG and McEver RP, Cloning of GMP-140, a granule membrane protein of platelets and endothelium: Sequence similarity to proteins involved in cell adhesion and inflammation. *Cell* **56:** 1033–1044, 1989.
17. Saijonmaa O, Nyman T, Hohenthal U and Fyhrquist F, Endothelin-1 is expressed and released by human endothelial hybrid cell line (EA.hy926). *Biochem Biophys Res Commun* **181:** 529–536, 1991.
18. Ziegler T, Silacci P, Harrison VJ and Hayoz D, Nitric oxide synthase expression in endothelial cells exposed to mechanical forces. *Hypertension* **32:** 351–355, 1998.
19. Lamas S, Marsden PA, Li EK, Tempst P and Michel T, Endothelial nitric oxide synthase: Molecular cloning and characterization of a distinct constitutive enzyme isoform. *Proc Natl Acad Sci USA* **89:** 6348–6352, 1992.
20. Gomex-Foix AM, Coats WS, Baque S, Alam T, Gerad RD and Newgard CB, Adenovirus-mediated transfer of muscle glycogen phosphorylase gene into hepatocytes confers altered regulation of glycogen metabolism. *J Biol Chem* **267:** 25129–25134, 1992.
21. Graham FL and van der Eb AJ, A new technique for the infectivity of human adenovirus 5 DNA. *Virology* **52:** 456–467, 1973.
22. Graham FL and Prevec L, Manipulation of adenovirus vectors. In: *Methods in Molecular Biology* (Ed. Murray EJ), Vol. 7, pp. 109–128. Humana, Clifton, 1991.
23. Kriegler M, *Gene Transfer and Expression*. Freeman, New York, 1990.
24. Laemmli UK, Cleavage of structural proteins during assembly of the head of bacteriophage T4. *Nature* **227:** 680–685, 1970.
25. Kuin A, Aaalders M, van der Valk MA, Frey A, Schmidt HHHW and Smets LA, Renal toxicity of the neuron blocking and mitochondriotropic agent *m*-iodobenzylguanidine. *Cancer Chemother Pharmacol* **42:** 37–45, 1998.
26. Bradford MM, A rapid and sensitive method for the quantitation of microgram quantities of protein utilizing the principle of protein–dye binding. *Anal Biochem* **72:** 248–254, 1976.
27. Schmidt HHHW, Pollock JS, Nakane M, Gorsky LD, Förstermann U and Murad F, Purification of a soluble isoform of

guanylyl cyclase-activating-factor synthase. *Proc Natl Acad Sci USA* **88:** 365–369, 1991.
28. Kantor DB, Lanzrein M, Stary SJ, Sandoval GM, Smith WB, Sullivan BM, Davidson N and Schuman EM, A role for endothelial NO synthase in LTP revealed by adenovirus-mediated inhibition and rescue. *Science* **274:** 1744–1748, 1996.
29. Cable DG, O'Brien T, Schaff HV and Pompili VJ, Recombinant endothelial nitric oxide synthase-transduced human saphenous veins. *Circulation* **96:** II-173–II-178, 1997.
30. Cable DG, O'Brien T, Kullo IJ, Schwartz RS, Schaff HV and Pompili VJ, Expression and function of a recombinant endothelial nitric oxide synthase gene in porcine coronary arteries. *Cardiovasc Res* **35:** 553–559, 1997.
31. Kullo IJ, Schwartz RS, Pompili VJ, Tsutsui M, Milstien S, Fitzpatrick LA, Katusic ZS and O'Brien T, Expression and function of recombinant endothelial NO synthase in coronary artery smooth muscle cells. *Arterioscler Thromb Vasc Biol* **17:** 2405–2412, 1997.
32. Ooboshi H, Chu Y, Rios CD, Faraci FM, Davidson BL and Heistad DD, Altered vascular function after adenovirus-mediated overexpression of endothelial nitric oxide synthase. *Am J Physiol* **273:** H265–H270, 1997.
33. Chen L, Daum G, Forough R, Clowes M, Walter U and Clowes AW, Overexpression of human endothelial nitric oxide synthase in rat vascular smooth muscle cells and in balloon-injured carotid artery. *Circ Res* **82:** 862–870, 1998.
34. Tsutsui M, Chen AFY, O'Brien T, Crotty TB and Katusic ZS, Adventitial expression of recombinant eNOS gene restores NO production in arteries without endothelium. *Arterioscler Throm Vasc Biol* **18:** 1231–1241, 1998.
35. Lowenstein CJ, Hill SL, Lafond-Walker A, Wu J, Allen G, Landavere M and Rose NR, Nitric oxide inhibits viral replication in murine myocarditis. *J Clin Invest* **97:** 1837–1843, 1996.
36. Karupiah G and Harris N, Inhibition of viral replication by nitric oxide and its reversal by ferrous sulfate and tricarboxylic acid cycle metabolites. *J Exp Med* **181:** 2171–2179, 1995.
37. Bi Z and Reiss CS, Inhibition of vesicular stomatitis virus infection by nitric oxide. *J Virol* **69:** 2208–2213, 1995.
38. Eissa NT, Yuan JW, Haggerty CM, Choo EK, Palmer CD and Moss J, Cloning and characterization of human inducible nitric oxide synthase splice variants: A domain, encoded by exons 8 and 9, is critical for dimerization. *Proc Natl Acad Sci USA* **95:** 7625–7630, 1998.
39. Xie Q, Leung M, Fuortes M, Sassa S and Nathan C, Complementation analysis of mutants of nitric oxide synthase reveals that the active site requires two hemes. *Proc Natl Acad Sci USA* **93:** 4891–4896, 1996.
40. Förstermann U, Boissel J-P and Kleinert H, Expressional control of the 'constitutive' isoforms of nitric oxide synthase (NOS-I and NOS-III). *FASEB J* **12:** 773–790, 1998.
41. Schaffner A, Blau N, Schneemann M, Steurer J, Edgell C-JS and Schoedon G, Tetrahydrobiopterin as another EDRF in man. *Biochem Biophys Res Commun* **205:** 516–523, 1994.
42. Janssens SP, Bloch KD, Nong Z, Gerad RD, Zoldhelyi P and Collen D, Adenoviral-mediated transfer of human endothelial nitric oxide synthase gene reduces acute hypoxic pulmonary vasoconstriction in rats. *J Clin Invest* **98:** 317–324, 1996.
43. Vaandrager AB, Smolenski A, Tilly BC, Houtsmuller AB, Ehlert EM, Bot AG, Edixhoven M, Boomaars WE, Lohmann SM and de Jonge HR, Membrane targeting of cGMP-dependent protein kinase is required for cystic fibrosis transmembrane conductance regulator Cl^- channel activation. *Proc Natl Acad Sci USA* **95:** 1466–1471, 1998.
44. Gambaryan S, Wagner C, Smolenski A, Walter U, Poller W, Haase W, Kurtz A and Lohmann SM, Endogenous or overexpressed cGMP-dependent protein kinases inhibit cAMP-dependent renin release from rat isolated perfused kidney, microdissected glomeruli, and isolated juxtaglomerular cells. *Proc Natl Acad Sci USA* **95:** 9003–9008, 1198.